Available online at www.sciencedirect.com

SCIENCE DIRECT

Developmental Biology 277 (2005) 102–113

DEVELOPMENTAL BIOLOGY

www.elsevier.com/locate/ydbio

The cellular and molecular etiology of the cleft secondary palate in *Fgf10* mutant mice

Sylvia R. Alappat[a,1], Zunyi Zhang[a,1], Kentaro Suzuki[b], Xiaoyun Zhang[a], Hongbing Liu[a], Rulang Jiang[c], Gen Yamada[b], YiPing Chen[a,d,*]

[a]*Division of Developmental Biology, Department of Cell and Molecular Biology, Tulane University, New Orleans, LA 70118, USA*
[b]*Center for Animal Resources and Development, Kumamoto University, Honjo 2-2-1, Kumamoto 860-0811, Japan*
[c]*Center for Oral Biology, University of Rochester Medical Center, Rochester, NY 14642, USA*
[d]*College of Bioengineering, Fujian Normal University, Fuzhou, Fujian Province, China*

Received for publication 23 March 2004, revised 12 August 2004, accepted 7 September 2004
Available online 2 October 2004

Abstract

Mammalian palatogenesis depends on interactions between the stomodium-derived epithelium and the cranial neural crest-derived ectomesenchyme. Fibroblast growth factor 10 (FGF10) is a mesenchymal signaling factor that guides the morphogenesis of multiple organs through tissue–tissue interactions. This is consistent with widespread agenesis and dysgenesis of organs observed in *Fgf10*$^{-/-}$ mice. In this study, we report the presence of a wide-open cleft secondary palate in *Fgf10* homozygous null mutant mice. *Fgf10* transcripts were detected in the palatal mesenchyme from E11.5 to E13.5 during normal palatogenesis and were enriched in the anterior and middle portions of the palatal shelves. In *Fgf10*$^{-/-}$ embryos, histological analyses revealed aberrant adhesion of the palatal shelves with the tongue in the anterior and fusion with the mandible in the middle and posterior beginning at E13.5, which could prevent normal elevation of the palatal shelves leading to a cleft palate. TUNEL and BrdU assays demonstrated significant levels of apoptosis in the medial edge epithelium (MEE) but unaltered cell proliferation in mutant palatal shelves. At the molecular level, we show that *Fgf10* is epistatic to *Jagged2* and *Tgfβ3* in the developing palate. Notably, the expression of *Jagged2* is downregulated throughout the palate epithelium in *Fgf10* mutants while *Tgfβ3* is misexpressed in the palatal epithelium at the oral side. Our results demonstrate that mesenchymally expressed *Fgf10* is necessary for the survival of MEE cells and for the normal expression of *Jagged2* and *Tgfβ3* in the palatal epithelium during mammalian palatogenesis.

Keywords: Cleft palate; Growth factor; *Fgf10*; *Jagged2*; *Tgfβ3*; Mouse

Introduction

The secondary palate develops from palatal shelves that emerge bilaterally from the internal surfaces of the maxillary primordia. The palatal shelves are formed of pharyngeal ectoderm and mesenchyme of both neural crest and mesodermal origin. Epithelial–mesenchymal interactions between the pharyngeal ectoderm and underlying mesenchyme guide the vertical growth of the palatal shelves on both sides of the tongue between embryonic day 12.0 (E12.0) and E13.5 in the mouse. Concomitant with the enlargement of the lower jaw and the lowering of the tongue at E14.0, the shelves elevate to a horizontal position above the dorsum of the tongue. Around E14.5, the horizontal palatal shelves make contact, adhere, and fuse along their midline forming a multilayered seam, which thins to a single layer and is eventually replaced by mesenchymal cells. This multistep palatogenesis is precisely regulated and coordinated. Disruption at any step of the process leads to the formation of cleft secondary palate.

* Corresponding author. Department of Cell and Molecular Biology, 2000 Precival Stern Hall, Tulane University, New Orleans, LA 70118. Fax: +1 504 865 6785.
E-mail address: ychen@tulane.edu (Y.P. Chen).
[1] These authors contributed equally to this work.

0012-1606/$ - see front matter © 2004 Elsevier Inc. All rights reserved.
doi:10.1016/j.ydbio.2004.09.010

Cleft palate is recognized as a commonly occurring congenital abnormality estimated as affecting 1/700 to 1/1000 births among European descent (Francis-West et al., 2003). The incidence of cleft palate varies widely depending upon genetic and environmental 'triggers' including exposure to teratogenic agents. Linkage disequilibrium studies on human syndromes with cleft palate and investigations of induced and spontaneous mouse mutants manifesting a secondary cleft palate have lead to the identification of genes and the developmental stage-specific aberrations associated with their mutant forms. The major categories recognized are (1) failure of palatal shelf formation or elevation exemplified by the human syndrome Treacher Collins, *Ryk* mouse mutants, *Ephb2/Ephb3* double mutant mice, *Pax9* mutant, and *Jagged2* mutant (Adams et al., 1999; Halford et al., 2000; Jiang et al., 1998; Orioli et al., 1996; Peters et al., 1998); (2) failure of shelves to meet and fuse following elevation as in the *Msx1* and *Osr2* mutants (Lan et al., 2004; Satokata and Maas, 1994); (3) persistence of the medial epithelial seam as reported in *Apaf1*-deficient mice, *Tgfß3* knockout mice, and *Egfr*$^{-/-}$ mice (Cecconi et al., 1998; Kaartinen et al., 1997; Martínez-Álvarez et al., 2000b; Miettinen et al., 1999; Taya et al., 1999), and (4) developmental defects of the tongue muscles featured in *Hoxa2* mutant mice that prevent descent of the tongue and block palate closure (Barrow and Capecchi, 1999).

Investigations into the cellular mechanisms underlying the disappearance of the midline epithelial seam provide evidence of cell intercalation (Tudela et al., 2002), programmed cell death (Cuervo and Covarrubias, 2004; Martínez-Álvarez et al., 2000b; Mori et al., 1994), cell migration (Carette and Ferguson, 1992), and epithelial–mesenchymal transformation (Griffith and Hay, 1992; Martínez-Álvarez et al., 2000b; Shuler et al., 1991, 1992). Recent studies by Cuervo and Covarrubias (2004) demonstrate that superficial peridermal cells migrate to the oral and nasal aspects allowing fusion of basal medial edge epithelium (MEE) cells from opposing shelves. Ultimately these basal cells undergo apoptosis in situ while periderm cells become apoptotic postmigration within the oral and nasal triangles of the midline epithelial seam. They found no evidence to support epithelial–mesenchymal transformation of MEE cells in the murine palate. Notably, activation of cell death triggers basal lamina degradation, a prerequisite for complete fusion and mesenchymal confluence (Blavier et al., 2001; Cuervo and Covarrubias, 2004). A 'cocktail' of metalloproteinases (MMPs) and tissue inhibitors of metalloproteinases (TIMPs) mediates the degradation of the basal lamina (Mansell et al., 2000; Morris-Wiman et al., 1999, 2000). Of the MMPs and TIMPs expressed in the developing palate, *MT1-Mmp*, *Mmp13*, and *Timp2* are expressed in the MEE during fusion (Blavier et al., 2001).

A growing number of genetic and environmental factors that are significant to the process of palate formation are being identified. Fibroblast growth factor 10 (FGF10) belongs to a family of more than 20 secreted polypeptide factors with essential roles in vertebrate embryogenesis and adult tissue homeostasis (reviewed in Ornitz and Itoh, 2001). FGF10 is a significant mediator of mesenchymal–epithelial signaling during vertebrate organogenesis through the regulation of cellular functions such as directed cell migration, cell proliferation, differentiation, and cell survival. Consistent with its widespread expression, mice lacking *Fgf10* exhibit agenesis and dysgenesis of multiple organs and die perinatally from respiratory failure (Min et al., 1998; Ohuchi et al., 2000; Sekine et al., 1999). In this study, we examined the expression pattern of *Fgf10* in the developing secondary palate and characterized the morphological, cellular, and molecular deviations between wild type and *Fgf10*-deficient palates that explain the cellular and molecular etiology of the cleft palate exhibited by *Fgf10*$^{-/-}$ mice.

Materials and methods

Animals

Generation and genotyping of *Fgf10*, *Jagged2*, and *Msx1* mutant mice have been described previously (Jiang et al., 1998; Satokata and Maas, 1994; Sekine et al., 1999). Mutant embryos were harvested from timed pregnant heterozygous mating. The embryonic age was defined as E0.5 in the morning of the day when a vaginal plug was discovered. Embryonic heads were removed and fixed in fresh 4% paraformaldehyde (PFA) in PBS overnight at 4°C, dehydrated through graded alcohol series, and embedded in paraffin for sectioning.

Histology and skeletal staining

Standard hematoxylin and eosin staining was performed on paraffin-embedded 10-μm coronal sections of staged embryonic heads from wild type and *Fgf10*$^{-/-}$ mice. Skeletal staining was done as previously described (Zhang et al., 2000). Briefly, the skin was removed from the heads of wild type and *Fgf10*$^{-/-}$ newborn mice and fixed successively in absolute ethanol and acetone for periods of 2 and 3 days, respectively. The fixed samples were stained in solution comprising 1:1:1:17 parts of 0.1% Alizarin Red S (in 95% ethanol):0.3% Alcian blue (in 70% ethanol):glacial acetic acid/ethanol for 5 days. Following alkaline hydrolysis and glycerol clearing, the differentially stained cartilage (blue) and bony (red) elements of the skull were visualized and photographed.

Cell proliferation and cell apoptosis assays

Immunodetection of BrdU on 10-μm paraffin-embedded samples was performed with the BrdU labeling and Detection Kit (Roche Diagnostics Corporation, Indianap-

olis) according to the manufacturer's protocol. Mouse embryos were labeled with BrdU via intraperitoneal injection of BrdU labeling reagent into timed pregnant mice. Embryos were fixed with Carnoy fixative 1 h after injection, dehydrated with ethanol, and embedded in wax. The primary and secondary antibody incubations were carried out at 37°C for 1 h and 30 min, respectively. Nitroblue tetrazolium/5-bromo-4-chloro-3-indolyl-phosphate (Roche Diagnostics Corp.) was used as substrate to visualize the sites of BrdU incorporation. The color reaction was performed at room temperature and in the dark.

TUNEL assay was performed using the 'In situ cell death detection kit' (Roche Diagnostics Corp.) following the manufacturer's instructions. Briefly, tissues were fixed in 4% PFA (in PBS) and then dehydrated through an increasing graded ethanol series and processed for sectioning. Following rehydration steps, the 10-μm sections were treated with Proteinase K (in 10 mM Tris–HCl, pH 8.0) at a concentration of 20 μg/ml for 15–20 min at room temperature. The samples were incubated with the TUNEL reaction mixture (a mixture of fluorescein-tagged nucleotides and the enzyme terminal deoxynucleotidyl transferase) at 37°C for 1 h and converter-AP (alkaline phosphatase conjugated to Antifluorescein Fab fragments) for 30 min at 37°C. NBT/BCIP was used as substrate solution to detect the sites of in situ apoptosis with a light microscope.

In situ hybridization

PFA-fixed samples (4%) were dehydrated by passage through a graded ethanol series. The dehydrated samples were subsequently embedded in paraffin in preparation for nonradioactive in situ hybridization. Serial tissue sections of 10-μm thickness were treated with proteinase K at 1 μg/ml for 20 min at room temperature. The following cDNAs were used to generate antisense riboprobes: an 800-bp mouse *Fgf10* (Suzuki et al., 2000); an 800-bp mouse *Msx1* (Hill et al., 1989); a 1.37-kb mouse *Pax9* (Peters et al., 1998); a 1.4-kb mouse *Jagged2* (Jiang et al., 1998); a 455-bp mouse *Tgfβ3* (from Invitrogen); a 470-bp mouse *Snail* (from Dr. Tom Gridley). The mouse *Fgfr2b*-specific cDNA (229 bp) and the 367-bp mouse *Tgfβ1* cDNA were cloned via RT-PCR. All riboprobes were generated by in vitro transcription using digoxigenin-UTP and according to the manufacturer's instructions (Roche Diagnostics Corp.). An anti-DIG alkaline phosphatase-conjugated antibody (Roche Diagnostics Corp.) was used to detect sites where probe bound. Visualization of the hybridization signal was accomplished by the addition of BM Purple AP substrate (Roche Diagnostics Corp.).

Results

Examination of *Fgf10* homozygous null neonates revealed a complete, wide-open cleft indicative of an abortive secondary palate development and failed separation of oral and nasal cavities unlike the wild type controls (Figs. 1A and B). Examination of skeletal preparations of wild type and *Fgf10*$^{-/-}$ heads of newborn mice revealed that the palatal processes of both the maxilla and palatine were absent allowing a direct view of the vomer and the presphenoid as illustrated in Figs. 1C and D.

We next examined the histological basis for a cleft palate phenotype in *Fgf10* null mutants. The first morphological aberration in palate development was evident as early as E12.5 but was pronounced by E13.5 (Fig. 2). At E12.5, the ventrolateral indentation of the shelf was poorly demarcated giving it a broadened appearance in the anterior and middle while posterior to the molars the shelves were narrow and wedge-shaped (data not shown). Histological examination of serial coronal sections through E13.5 mutant heads revealed occasional adhesion of the palatal shelf with the tongue in the anterior and recurrent fusion with the

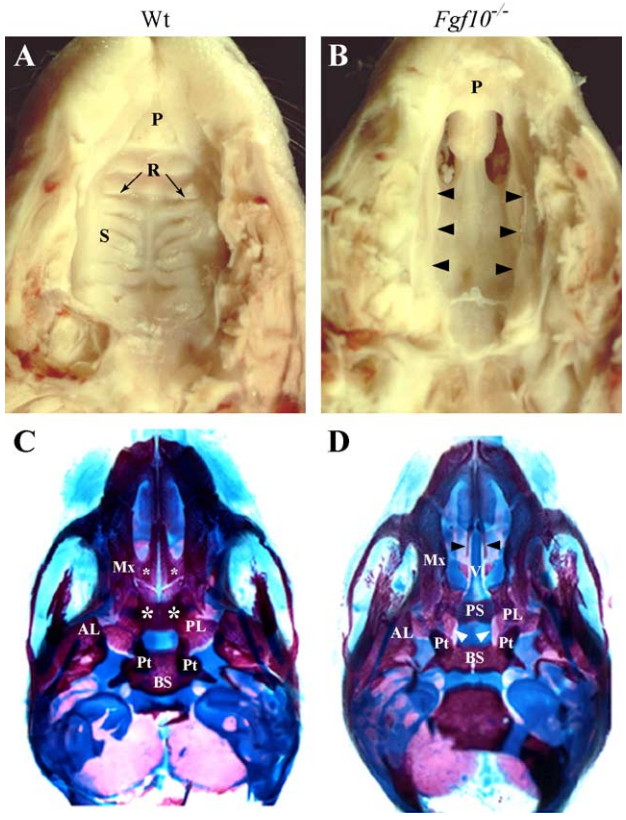

Fig. 1. *Fgf10*$^{-/-}$ mice exhibit a complete cleft secondary palate. (A) An oral view of a normal palate of a newborn wild type mouse. (B) A wide-open secondary cleft palate (black arrowheads) of a newborn *Fgf10*$^{-/-}$ mouse. (C and D) Stained skeletal preparations of neonatal skulls. Ventral view of the skull in normal (C) and *Fgf10*$^{-/-}$ mice (D). In the mutant, the palatal shelves of the maxilla (Mx) are absent while the vestigial shelves of the palatine (PL) appear to be laterally displaced (white arrow heads) allowing direct viewing of the vomer (v) and presphenoid (PS) skull bone elements. In C, small asterisks represent shelves of the maxilla and large asterisks indicate shelves of the palatine. Black arrowheads in D indicate the vestiges of the maxilla in the mutants. Abbreviation: P, primary palate; R, rugue; S, secondary palate; AL, alisphenoid; BS, basisphenoid; Pt, pterygoid.

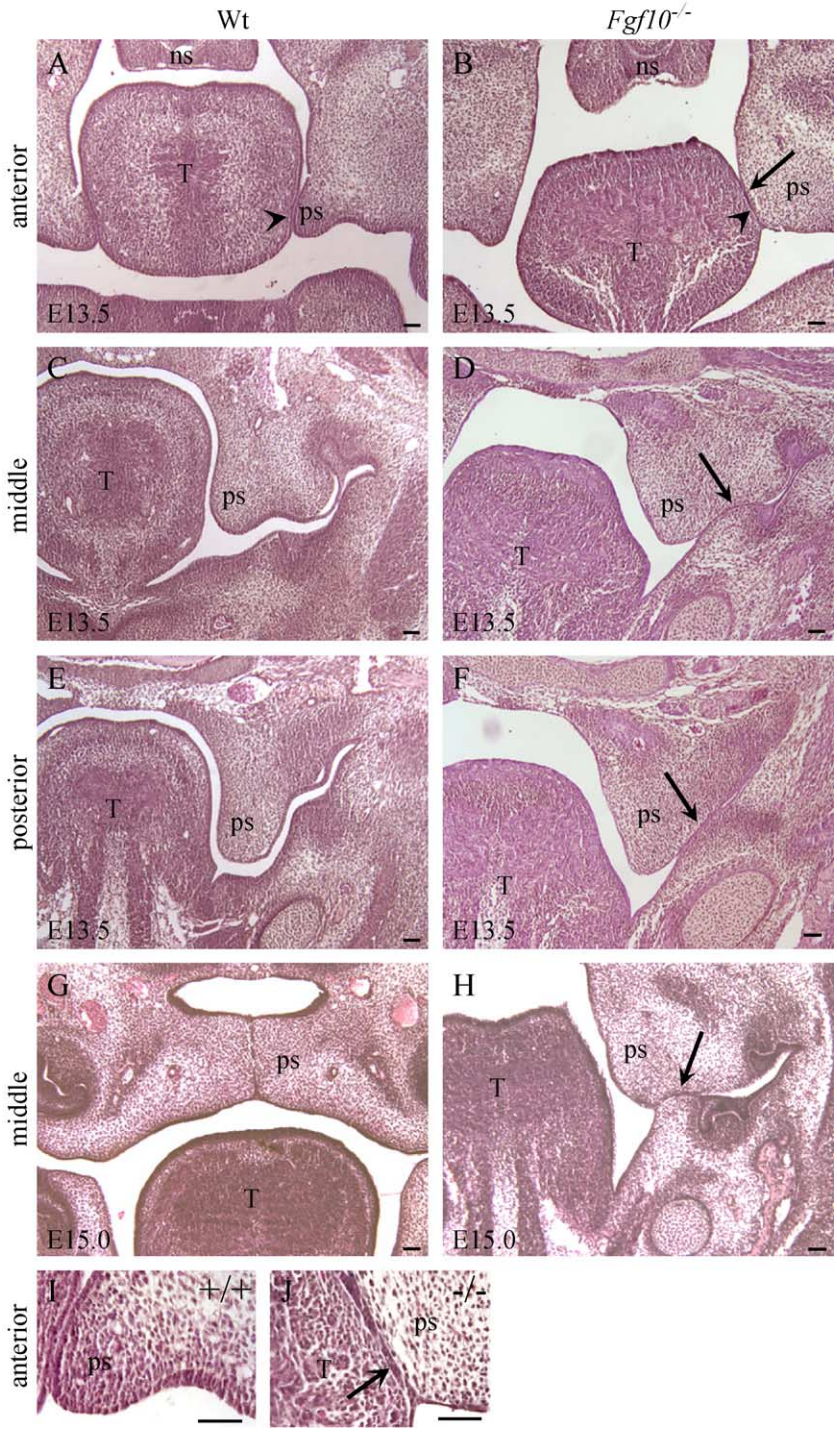

Fig. 2. Histological analyses of coronal sections of wild type and *Fgf10*$^{-/-}$ palates at E13.5 (A–F) and E15.0 (G and H). (A and B) Sections anterior to the first molars; (C, D, G, and H) sections along the plane of the first molars designated as middle portion; (E and F) sections posterior to the first molars. (I and J) Magnified view of the region indicated by an arrowhead in panels A and B. The arrows in B and J point to the site of adhesion between the anterior palate and the tongue in the mutants. The arrows in D, F, and H point to anomalous fusion of the oral epithelia of the palate and the mandible. (G and H) Bilateral shelf elevation is impaired in *Fgf10*$^{-/-}$ mutant mice. (G) At E15.0, the palatal shelves from wild-type embryos have elevated and are horizontally oriented over the dorsum of the tongue as seen in coronal sections through the middle plane. (H) Palatal shelves from a corresponding stage in null mutant embryos fail to elevate and remain vertically oriented. Abbreviation: ns, nasal septum; ps, palatal shelf; T, tongue. Scale bars in A–F = 50 μm.

mandible in the middle and posterior planes (Figs. 2B, D, F, and J). At E14.5–15.0 while the palatal shelves in wild type had elevated to a position above the dorsum of the tongue, the mutant shelves remained in vertical orientation on either side of the tongue (Fig. 2H). Thus, in *Fgf10* null mutants, the elevation of the palatal shelves was physically prevented

by adhesion or fusion to the tongue and mandible along their nasal and oral aspects. Consequently, the tongue never descends in *Fgf10* mutants.

The presence of a cleft palate in *Fgf10*$^{-/-}$ mice suggests that *Fgf10* plays a critical role in palate development. To determine the correlation between *Fgf10* expression and the different stages of palatal morphogenesis, we analyzed the spatiotemporal distribution of *Fgf10* transcripts in the palate from E11.5 to E14.5 embryos (Fig. 3). *Fgf10* was exclusively found in the palatal mesenchyme from E11.5 to E13.5. Interestingly, *Fgf10* was expressed in close apposition to the palatal epithelium in the anterior through middle planes at E11.5 when palate development initiates with little to no expression posterior of the first molars (Figs. 3A, D, and G). By E12.5 and E13.5, expression was displaced gradually ventrolaterally away from the MEE and was detected in close apposition to the oral epithelium occupying the mid-oral and lateral regions of the palate mesenchyme (Figs. 3B, C, E, and F). *Fgf10* expression was greatly reduced in the posterior palate and showed maximal displacement into the lateral mesenchyme just outside of the palatal shelves (Figs. 3H and I). No *Fgf10* expression was detected at E14.5 (data not shown). In addition to the palate, *Fgf10* was expressed in the mesenchyme of the tongue in a decreasing anterior–posterior and distal–proximal gradient from E11.5 to 13.5. The expression in the tongue was most intense in the anterior planes at E12.5 and E13.5 (Figs. 3B and C).

FGF10 is a secreted signaling factor with established roles in organogenesis. At the cellular level, FGF10 functions either to promote the proliferation of the epithelial components in developing organ primordia such as the lungs, pancreas, and cecum, or imparts a survival function as reported in the incisor tooth germs (Bellusci et al., 1997; Bhushan et al., 2001; Burns et al., 2004; Harada et al., 2002; Hart et al., 2003). Therefore, we hypothesized that loss of *Fgf10* function may result in cell proliferation or survival defects leading to aberrant extension of the palate. We compared cell proliferation rates between the wild type and *Fgf10* mutant palates at E12.5 using BrdU incorporation assays (Figs. 4A–D). The results revealed comparable levels of cell proliferation in wild type and mutant samples

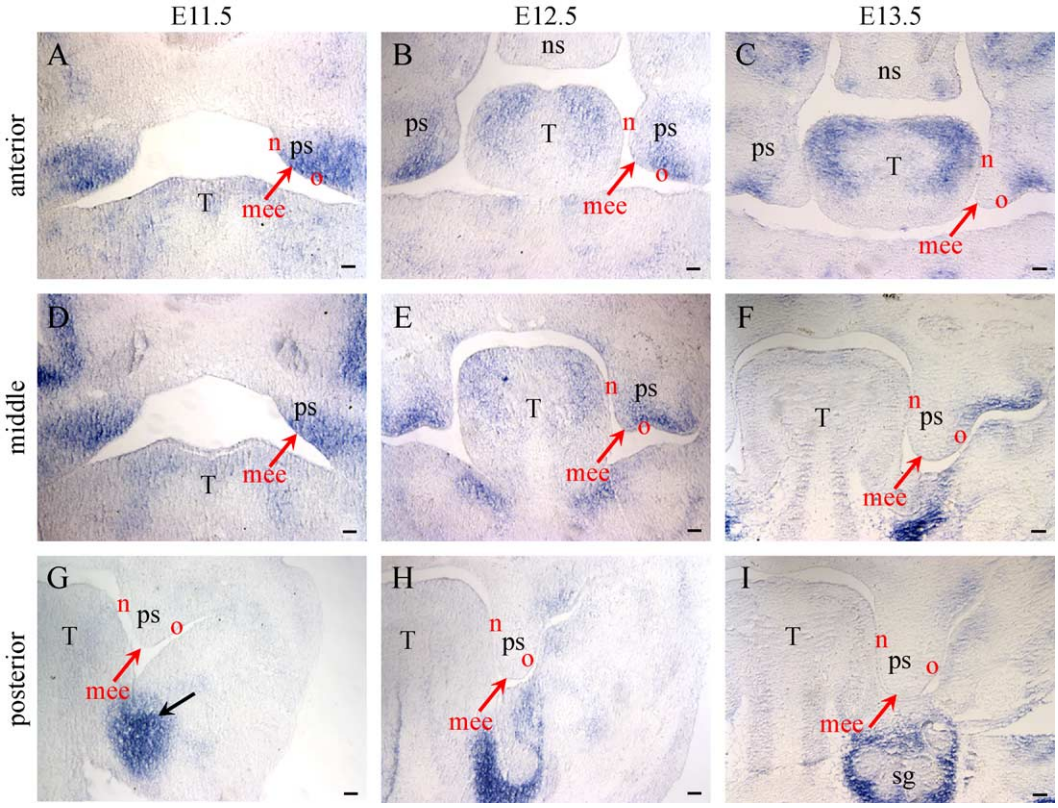

Fig. 3. *Fgf10* expression in developing palatal shelves. (A–C) Coronal sections of the palatal shelves anterior to the first molars. (D–F) Coronal sections of the palatal shelves along the plane of the first molars. (G–I) Coronal sections of the palatal shelves posterior to the first molars. (A, D, and G) At E11.5, *Fgf10* is intensely expressed in the mesenchyme of the developing palatal shelves in the anterior (A) and middle (D) portions in close apposition to the medial edge epithelia. Expression is also seen in the forming tongue. However, *Fgf10* expression is not evident in the posterior palatal shelves, but is present in the submandibular gland anlage (arrow) (G). (B, E, and H) By E12.5, the *Fgf10* expression domain is displaced ventrolaterally away from the MEE but subjacent to the oral epithelia of the palate (B and E). Expression in the tongue is stronger in the anterior–dorsal regions. (B and E) Faint expression of *Fgf10* is seen lateral to the ventral indentation (H). *Fgf10* expression also localizes to the mesenchymal component of the submandibular gland primordial (H). (C, F, and I) At E13.5, maximal ventrolateral displacement of *Fgf10* expression is observed, which spans the midoral to lateral mesenchyme in all planes examined. Expression in the submandibular gland persists (I). Abbreviation: mee, medial edge epithelium; n, nasal; ns, nasal septum; o, oral; ps, palatal shelf; sg, submandibular gland; T, tongue. Scale bars A–I = 50 μm.

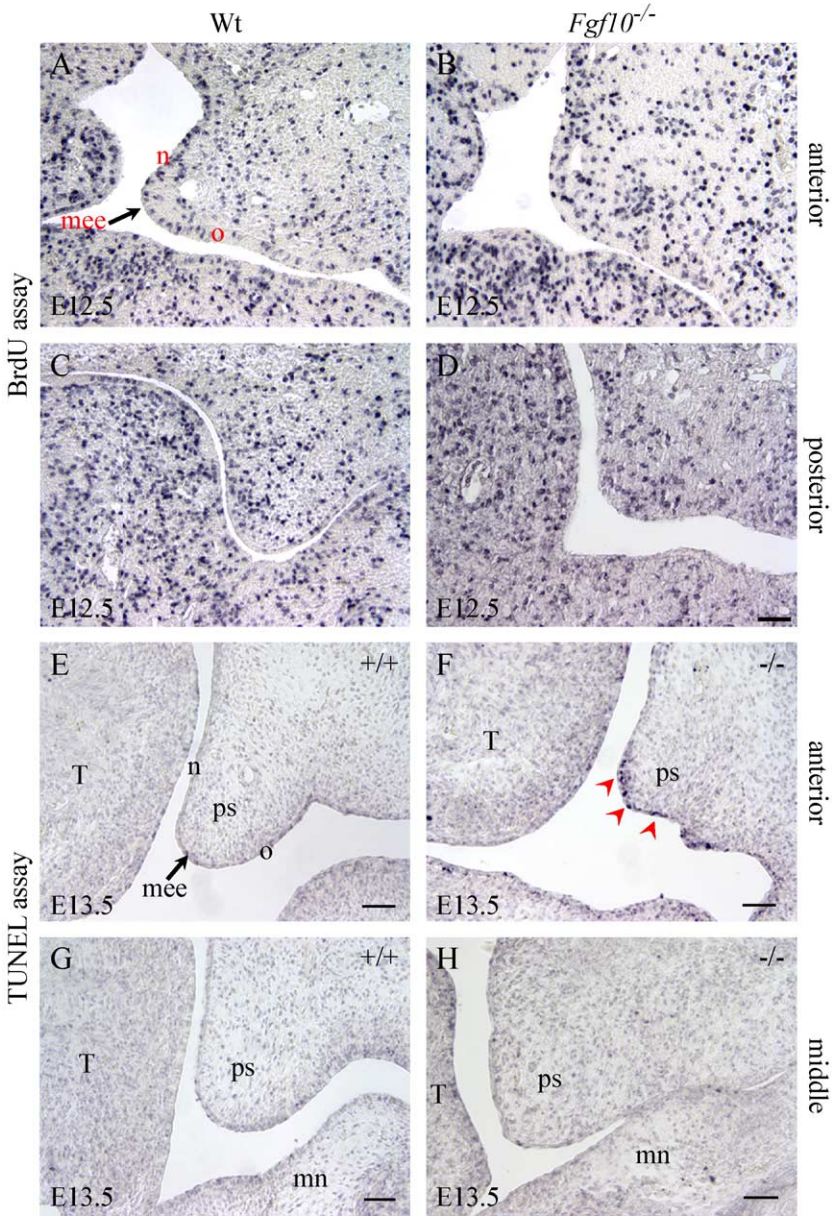

Fig. 4. Analyses of cell proliferation and apoptosis in *Fgf10*$^{-/-}$ palatal shelves. (A–D) Cell proliferation assays on E12.5 palatal shelves of wild type (A and C) and *Fgf10* mutant (B and D) mice show comparable levels of cell proliferation in the anterior (A and B) and posterior (C and D) portions of palate. (E–H) TUNEL assays on E13.5 palatal shelves of wild type (E and G) and *Fgf10* mutants (F and H) show significant cell apoptosis in the anterior medial edge epithelium of the mutant palate (arrows) (B). Abbreviation: mee, medial edge epithelium; mn, mandible, n, nasal; o, oral; ps, palatal shelf, T, tongue. Scale bars = 50 μm.

throughout the palate. However, TUNEL assays on coronal sections of E13.5 wild type and mutant heads showed significant levels of cell apoptosis within the anterior MEE cells of the mutant palatal shelves (Figs. 4E–H). The posterior region of the palatal shelves in mutants, similar to the wild type controls, did not show cell apoptosis. Therefore, during palatogenesis, FGF10 functions as a survival factor for the anterior MEE. Given that mesenchymal expression of *Fgf10* was not seen in close apposition to the MEE at this stage, it would appear that the survival function is indirect.

To understand the molecular epistatic relationships within the FGF10 signaling pathway and the genes thought to be critical for normal palatogenesis, we compared the distribution of certain candidate genes in the developing palates of wild-type embryos and *Fgf10* homozygous null mutants. Previous studies have shown strong induction of *Pax9* by FGF8 in explants of the posterior palate (Zhang et al., 2002). Moreover, it was reported that *Pax9* deficiency results in unelevated palatal shelves owing to a mechanical hindrance (Peters et al., 1998). Similar to *Fgf10*$^{-/-}$ mice, the shelves in *Pax9* mutants are abnormally shaped and lacked the characteristic ventrolateral indentation. Therefore, we asked if *Pax9* is a candidate gene in the FGF10 signaling pathway. Accordingly, we examined the levels of

Pax9 expression in the palate from *Fgf10* null embryos and found that its distribution was unaltered from wild type (Fig. 5). The *Msx1* homeobox gene is exclusively expressed in the anterior mesenchymal cells of the developing palate and controls a genetic pathway that includes *Shh*, *Bmp2*, and *Bmp4* (Zhang et al., 2002). To test if *Msx1* and *Fgf10* exist in the same genetic pathway, we examined *Msx1* expression in $Fgf10^{-/-}$ palate as well as *Fgf10* expression in $Msx1^{-/-}$ palate. The results indicated an unchanged *Msx1* expression in *Fgf10* mutants and vice versa, as compared to that in the wild-type palate (data not shown). In addition, although FGF receptor-2b (FGFR2b) functions as a receptor for the FGF10 ligand (Igarashi et al., 1998) and knockout of *Fgfr2b* in mice similarly results in a cleft palate (De Moerlooze et al., 2000), *Fgfr2b* expression, which is detected in the palatal epithelium, remains unaltered in the developing palatal shelves of $Fgf10^{-/-}$ embryo (data not shown). We therefore conclude that *Pax9*, *Msx1*, and *Fgfr2b* are not downstream target genes of FGF10.

Null mutants of the gene encoding the Notch ligand Jagged2 give a palate phenotype similar to *Fgf10* mutants. Embryos deficient in *Jagged2* develop a cleft palate as a result of failed elevation of palatal shelves that are aberrantly adhered or fused with the tongue and the mandible (Jiang et al., 1998). Previous studies have demonstrated that FGF10 can positively regulate the expression of various members of the Notch signaling pathway among them *Jagged2* in the developing pancreas (Norgaard et al., 2003). This regulation of Notch signaling by FGF10 dictates cell proliferation versus cell differentiation decisions within a population of pancreatic progenitor cells (Hart et al., 2003; Norgaard et al., 2003). In addition, integration of FGF10 and Notch signaling pathways is used in establishing the stem cell compartment of mouse incisors and in specifying tissue boundaries of the enamel knot within the molars (Harada et al., 1999; Mustonen et al., 2002). Given the similarity of the cleft palate phenotype between *Jagged2* and $Fgf10^{-/-}$ mutants together with evidence supporting the integration of FGF10 and Notch pathways within other developing organs, we examined the expression of *Jagged2* in the $Fgf10^{-/-}$ palate. In situ hybridization revealed that *Jagged2* was expressed throughout the epithelium of a wild-type palate at E12.5 (Figs. 6A, C, and E). Significantly, in the *Fgf10* mutant, we

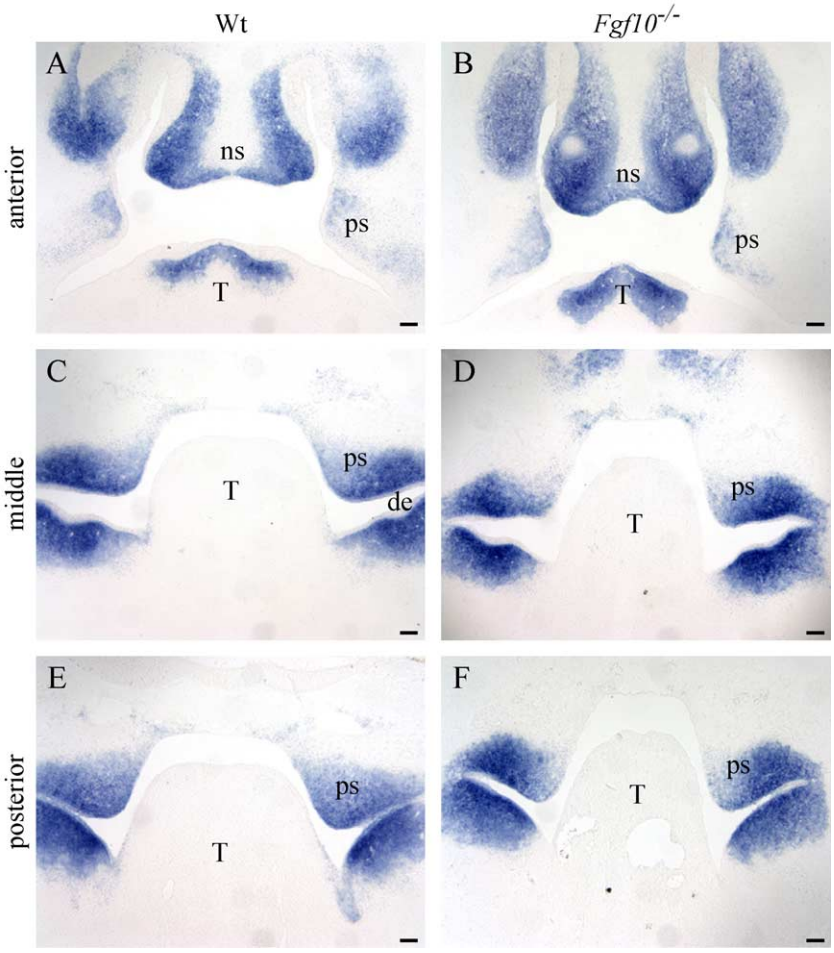

Fig. 5. Expression of *Pax9* in wild type and $Fgf10^{-/-}$ palatal shelves at E12.5. The *Fgf10* mutants (B, D, and F) show comparable expression levels and patterns of *Pax9* to the wild type (A, C, and E) in the anterior (A and B), middle (C and D), and posterior planes (E and F). Abbreviation: de, dental epithelium; ns, nasal septum; ps, palatal shelf; T, tongue. Scale bars = 50 μm.

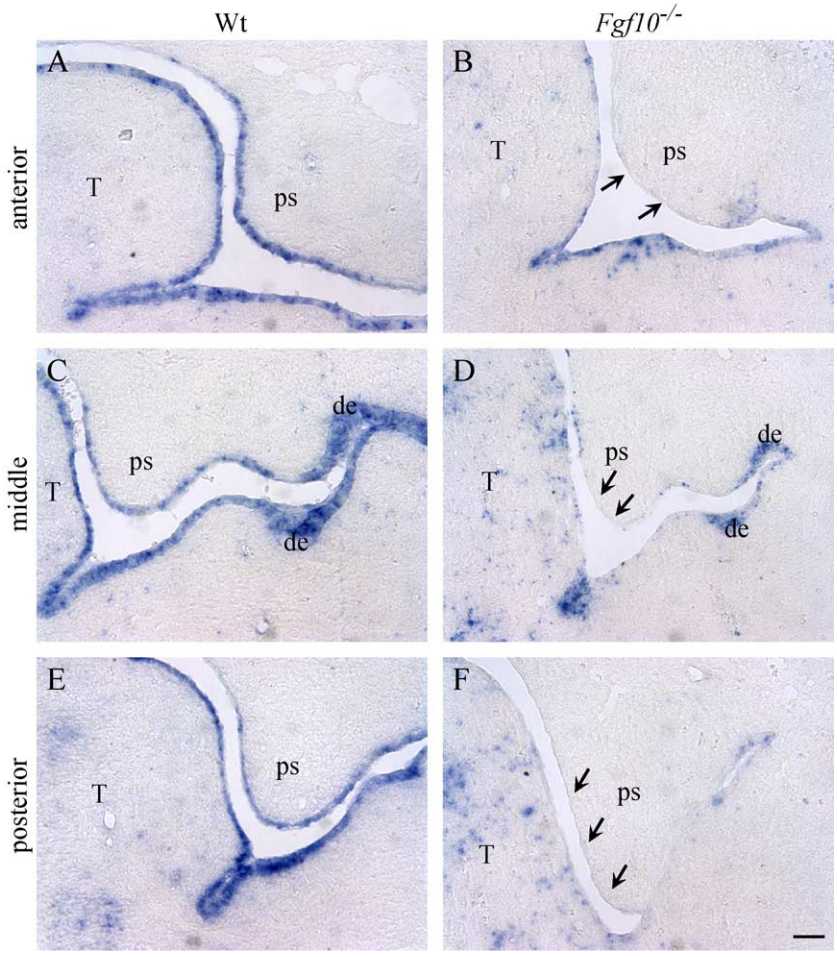

Fig. 6. Downregulation of *Jagged2* expression in *Fgf10*$^{-/-}$ palatal shelves. (A, C, and E) *Jagged2* is expressed in the nasal, oral, and medial edge epithelia of the wild type palate at E12.5. (B, D, and F) Significant downregulation of *Jagged2* expression is seen in the palate epithelium (arrows) of *Fgf10*$^{-/-}$ mutant embryo at E12.5. Abbreviation: de, dental epithelium; ps, palatal shelf, T, tongue. Scale bar = 50 μm.

found a complete downregulation of *Jagged2* expression throughout the palate epithelium at the equivalent stage (Figs. 6B, D, and F), but *Jagged2* expression in the dental epithelium remained unaltered (Fig. 6D). Our results indicate that *Fgf10* is epistatic to *Jagged2* in the developing palate. This conclusion is further supported by evidence that *Fgf10* expression remains unaltered in *Jagged2* mutants (data not shown).

Beginning at E13.5, we observed anomalous fusion of the palatal shelves with the mandible in the middle and posterior regions of the *Fgf10*$^{-/-}$ mutant palate. Several studies support a critical role for TGFβ3 in the process of normal palate fusion involving the MEE. Also, *Tgfβ3* expression is specifically confined to the MEE in the wild type palate (Fitzpatrick et al., 1990; Pelton et al., 1990). We asked if the fusion between the oral epithelia of the palate and the mandible in the *Fgf10* mutant involved ectopic *Tgfβ3* expression. We checked the mutant palates for *Tgfβ3* expression and compared the transcript distribution patterns with that of wild type (Fig. 7). Remarkably, while the anterior showed similar expression pattern, in the middle and posterior planes we detected ectopic expression of *Tgfβ3* in the oral epithelium of the palate and at the site of fusion between the palatal shelves and mandible. Therefore, *Fgf10* regulates *Tgfβ3* and the misexpression of *Tgfβ3* in *Fgf10*$^{-/-}$ null mutants partially explains the aberrant fusion seen between the mandible and the oral epithelium of the palatal shelves. Further substantiating this conclusion was the detection of apoptotic cells along the fusion site at E15.5 (Figs. 7G and H) and the emerging confluence of the palate with the mandible beginning at E16.5 (Fig. 7I). To examine if a downregulation of *Jagged2* in the *Fgf10*$^{-/-}$ palatal epithelium accounts for the ectopic *Tgfβ3* expression, we examined *Tgfβ3* expression in *Jagged2* mutants at E13.5. Contrary to our expectations, we found no alteration in *Tgfβ3* expression in *Jagged2* mutants when compared with wild-type controls (data not shown). Therefore, our data suggest that FGF10 regulates *Jagged2* and *Tgfβ3* by two discrete pathways.

A correlation between apoptosis in the MEE and the expression of *Tgfβ3*, *Tgfβ1*, and *Snail* has been recently demonstrated (Martínez-Álvarez et al., 2004). A lack of *Tgfβ3* expression in the MEE leads to upregulation of *Tgfβ1* in the palatal mesenchyme. An elevated *Tgfβ1* in turn

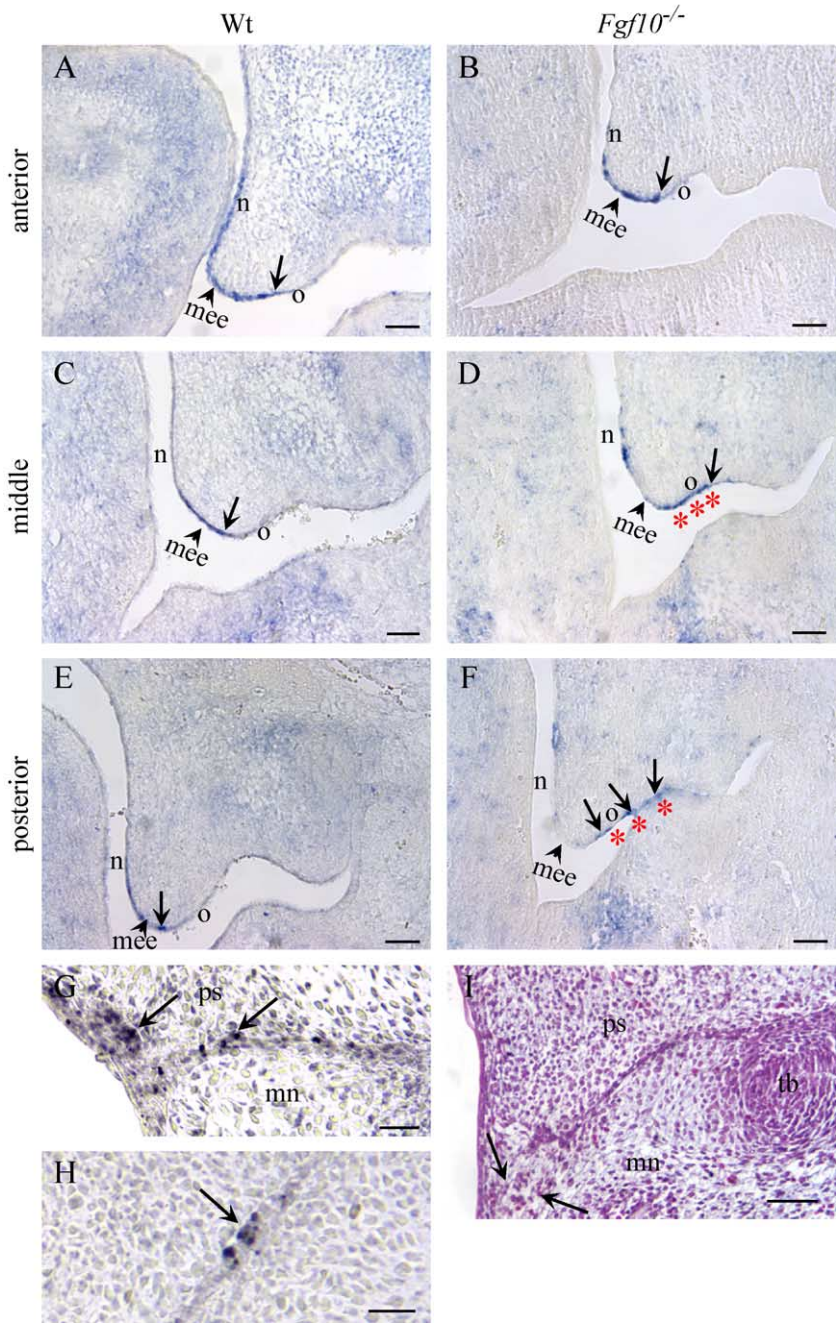

Fig. 7. Ectopic expression of *Tgfβ3* in *Fgf10*$^{-/-}$ palates at E13.5. (A, C, and E) Wild-type expression of *Tgfβ3* in the palatal epithelium of anterior (A), middle (C), and posterior (E) planes. (B, D, and F) Expression of *Tgfβ3* in the palatal epithelium of the mutant palate. Expression in the anterior plane (B) is comparable to the wild type, but the expression in the middle (D) and posterior (F) planes expanded to the oral side. Arrows indicate the extent of *Tgfβ3* expression. (G and H) TUNEL-positive cells are detected at the site of fusion between the palatal epithelium and the mandibular epithelium. (I) Coronal section of *Fgf10*$^{-/-}$ palate at E16.5 shows fusion of the palatal shelf with the mandible in the middle portion of palate. The black arrows point to the site of mesenchymal confluence. Abbreviation: mee, medial edge epithelium; mn, mandible; n, nasal; o, oral; ps, palatal shelf; tb, tooth bud. The red asterisks in panels D and F indicate ectopic sites of *Tgfβ3* expression. Scale bars = 50 μm.

activates ectopic *Snail* expression in the palatal epithelium and promotes cell survival (Martínez-Álvarez et al., 2004). We asked whether ectopic *Tgfβ3* expression in the palatal epithelium of *Fgf10*$^{-/-}$ mice suppresses the expression of *Tgfβ1* and *Snail* in the palatal mesenchyme, which may also contribute to the high levels of cell apoptosis observed in the MEE and at the sites of aberrant fusion between the palatal shelves and mandibles of *Fgf10* mutants. In situ hybridization analyses revealed that the levels of *Tgfβ1* and *Snail* expression in the palates of *Fgf10*$^{-/-}$ mice were comparable to that of wild type (data not shown), thus ruling out this possibility.

Discussion

This study examines the role of FGF10 in palate development and attempts to elucidate the cellular and molecular basis for a cleft palate phenotype in *Fgf10*$^{-/-}$ mutant mice. We have shown that *Fgf10* mutants have a complete cleft secondary palate by examining the gross morphology and by skeletal staining. Histological analyses reveal that these mutants have an elevation defect caused by the anomalous fusion of the palatal shelves with the tongue in the anterior and the mandible in the middle to posterior regions. We have also shown that *Fgf10* was expressed from E11.5 to E13.5 by in situ hybridization and that it may be indirectly required for the survival of medial edge epithelial cells in the anterior regions of the developing palate. Lastly, we demonstrate that FGF10 regulates the expression of *Jagged2* and *Tgfβ3* by two separate pathways.

Our results demonstrate that both *Jagged2* and *Tgfβ3* function downstream of *Fgf10* during palatogenesis. In the *Fgf10* homozygous null embryos, *Jagged2* expression was completely lost from the palate while *Tgfβ3* was ectopically expressed in the mutant palate epithelium with its expression domain extending past the medial edge epithelium into the oral and nasal epithelia (Figs. 6 and 7). Therefore, *Fgf10* positively regulates *Jagged2* and negatively regulates *Tgfβ3.* The observed fusion of the palatal shelves with the tongue and mandible in *Fgf10*$^{-/-}$ palate probably occurs as a result of downregulation of *Jagged2* compounded by the ectopic expression of *Tgfβ3*, both of which appear to be independently regulated by *Fgf10*. *Jagged2* and *Tgfβ3* represent critical factors in palatogenesis since targeted deletion of either gene results in a cleft palate. As in teeth, we demonstrate a survival function for *Fgf10* in the palate. Loss of *Fgf10* results in apoptosis of medial edge epithelial cells in the anterior. This is consistent with the observed expression of *Fgf10* in the anterior and middle regions of the palate mesenchyme.

Positive regulation of genes in the Notch pathway by FGF10 was previously reported in the tooth and pancreas (Hart et al., 2003; Mustonen et al., 2002). In addition to the palate, *Jagged2* and *Fgf10* are expressed in the limb, submandibular glands, and tooth where epithelial–mesenchymal interactions drive organogenesis (Valsecchi et al., 1997). The possibility of any interaction between Jagged2 and TGFβ3 signaling in the palate falls outside the scope of the present study. However, the literature supports the existence of cross talk between the Notch and TGFβ pathways in myogenic, endothelial, pancreatic, and neuronal development (Goumans et al., 2002; Kim and Hebrok, 2001; Shah et al., 1996). In these instances, intracellular transducers of both pathways are recruited to promoters on Notch target genes through protein–protein interactions leading to signal integration (Blokzijl et al., 2003).

Ferguson (1984) reported that the adhesion of the palatal shelves exhibited tissue specificity and normally occurs between the medial edge epithelia and not the tongue or superficially placed maxillary epithelia. In *Fgf10*$^{-/-}$ mutants, we find the aberrant bilateral fusion of the palatal shelves with the mandible in the middle and posterior regions (Fig. 2). Since TGFβ3 is essential for the adhesion and fusion of the contacting palatal shelves, we hypothesized that the aberrant fusion between the oral epithelium of the palatal shelves and the mandible in the *Fgf10*$^{-/-}$ mutants could be the result of ectopic expression of *Tgfβ3.* The biological roles of TGFβ3 in the developing palate are many. It is required for maintaining MEE cell polarity, the induction of cellular appendages that promote adhesion, and the regulation of cell intercalation, cell death, and EMT to form the definitive palate (Gato et al., 2002; Kaartinen et al., 1997; Martínez-Álvarez et al., 2000a,b; Taya et al., 1999; Tudela et al., 2002). Examination of *Tgfβ3* expression between wild type and *Fgf10*$^{-/-}$ palate at E13.5 revealed that *Tgfβ3* expression extends into the oral epithelium in the middle and posterior regions of mutant palatal shelves. The expression in the anterior regions remained confined to the medial edge epithelia and is comparable between mutants and wild type samples. Histological sections through the E16.5 *Fgf10*$^{-/-}$ palate revealed thinning and gradual disappearance of the epithelium along the line of fusion (Fig. 7I), consistent with the known function of *Tgfβ3*. This, together with the observed TUNEL-positive cells also at the site of aberrant fusion, gives credence to our hypothesis. Thus, the absence of FGF10 results in the misexpression of *Tgfβ3* rendering the oral epithelia competent to fuse with the mandible. To date, the literature supports both synergistic and antagonistic interactions between the FGF and TGFβ family members when modulating various developmental events (Papetti et al., 2003; Unda et al., 2001). Our study suggests that FGF10 exerts a molecular control on the temporospatial expression of *Tgfβ3* within medial edge epithelial cells.

In a normally developing palate, *Tgfβ3* expression is first seen at E13.5 in the MEE (Fitzpatrick et al., 1990; Pelton et al., 1990). Our study shows that as palatal development progressed, *Fgf10* expression in the mesenchyme became more and more ventrolaterally displaced. The emergence of *Tgfβ3* expression around E13.5 appears to coincide with the displacement of *Fgf10* expression away from the MEE. Furthermore, the extended domain of *Tgfβ3* expression in the oral palatal epithelia of *Fgf10* homozygous null mutants suggests a negative influence of *Fgf10* on *Tgfβ3* during palatal ontogeny. Therefore, the temporal and spatial expression of *Fgf10* may serve as a molecular control for the timely expression of *Tgfβ3* at late E13.5 when *Fgf10* expression in the wild type palate begins to decline and becomes ventrolaterally displaced probably permitting the induction of *Tgfβ*3 expression in the MEE. This is reminiscent of the role of FGF10 in the developing lungs where it functions as a morphogen in regulating the spatial expression of genes (Bellusci et al., 1997; Park et al., 1998; Weaver et al., 2000).

Both *Fgf10* and *Jagged2* null mice exhibit wide-open clefts as a result of impaired elevation of the palatal shelves. In both these mutants, the palate adheres dorsally with the tongue. The fusion of the palate with the mandible is more pronounced in the *Fgf10* mutant and extends from the middle to the posterior of the palate, while in *Jagged2* mutants fusion with the mandible is regionally restricted to the medial, mid-oral plane. Comparable levels of *Fgf10* expression in *Jagged2* homozygous mutants and in wild type embryos confirm that mesenchymal *Fgf10* is epistatic to epithelial *Jagged2* in the developing palate (data not shown). Contrary to our expectation, misexpression of *Tgfβ3* is specific to *Fgf10* mutant palates and is not observed in the *Jagged2*$^{-/-}$ palate. The expression of *Tgfβ3* in *Jagged2* null background was similar to that in wild type. Together, our studies indicate that the down-regulation of *Jagged2* and the extended domain of *Tgfβ3* expression in the *Fgf10* mutant result in a more pronounced elevation defect. This could account for the more aggressive fusion observed between the palate and mandible in *Fgf10*$^{-/-}$ mutants as opposed to *Jagged2*$^{-/-}$ mutants.

The combined regulation of Notch and TGFβ signaling pathways by FGF10 appears to be essential to a normally developing palate. Further elucidation of the molecular hierarchies and the cellular responses evoked by cross talk between these pathways will contribute significantly to our understanding of the etiology of a cleft palate.

During the revision of this paper, similar results from studies on *Fgf10*$^{-/-}$ mice were reported by Rice et al. (2004). The authors also demonstrated that *Shh* in the palatal epithelium is a downstream target of FGF10 signaling. However, the authors showed a decreased cell proliferation in *Fgf10*$^{-/-}$ palatal epithelium, a phenotype that we did not observe.

Acknowledgments

This work was supported by NIH grants (R01DE14044, R01DE12329) and the Millenium Trust Health Excellence Fund (HEF-2000-05-04) from the Louisiana Board of Regents to Y.P.C.

References

Adams, R.H., Wilkinson, G.A., Weiss, C., Diella, F., Gale, N.W., Deutsch, U., Risau, W., Klein, R., 1999. Roles of ephrinB ligands and EphB receptors in cardiovascular development: demarcation of arterial/venous domains, vascular morphogenesis, and sprouting angiogenesis. Genes Dev. 13, 295–306.

Barrow, J.R., Capecchi, M.R., 1999. Compensatory defects associated with mutations in *Hoxa1* restore normal palatogenesis to *Hoxa2* mutants. Development 126, 5011–5026.

Bellusci, S., Grindley, J., Emoto, H., Itoh, N., Hogan, B.L., 1997. Fibroblast growth factor 10 (FGF10) and branching morphogenesis in the embryonic mouse lung. Development 124, 4867–4878.

Bhushan, A., Itoh, N., Kato, S., Thiery, J.P., Czernichow, P., Bellusci, S., Scharfmann, R., 2001. *Fgf10* is essential for maintaining the proliferative capacity of epithelial progenitor cells during early pancreatic organogenesis. Development 128, 5109–5117.

Blavier, L., Lazaryev, A., Groffen, J., Heisterkamp, N., DeClerck, Y.A., Kaartinen, V., 2001. TGF-beta3-induced palatogenesis requires matrix metalloproteinases. Mol. Biol. Cell 12, 1457–1466.

Blokzijl, A., Dahlqvist, C., Reissmann, E., Falk, A., Moliner, A., Lendahl, U., Ibanez, C.F., 2003. Cross-talk between the Notch and TGF-beta signaling pathways mediated by interaction of the Notch intracellular domain with Smad3. J. Cell Biol. 163, 723–728.

Burns, R.C., Fairbanks, T.J., Sala, F., De Langhe, S., Mailleux, A., Thiery, J.P., Dickson, C., Itoh, N., Warburton, D., Anderson, K.D., Bellusci, S., 2004. Requirement for fibroblast growth factor 10 or fibroblast growth factor receptor 2-IIIb signaling for cecal development in mouse. Dev. Biol. 265, 61–74.

Carette, M.J., Ferguson, M.W., 1992. The fate of medial edge epithelial cells during palatal fusion in vitro: an analysis by DiI labelling and confocal microscopy. Development 114, 379–388.

Cecconi, F., Alvarez-Bolado, G., Meyer, B.I., Roth, K.A., Gruss, P., 1998. Apaf1 (CED-4 homolog) regulates programmed cell death in mammalian development. Cell 94, 727–737.

Cuervo, R., Covarrubias, L., 2004. Death is the major fate of medial edge epithelial cells and the cause of basal lamina degradation during palatogenesis. Development 131, 15–24.

De Moerlooze, L., Spencer-Dene, B., Revest, J.-M., Hajihosseini, M., Rosewell, I., Dickson, C., 2000. An important role for the IIIb isoform of fibroblast growth factor receptor 2 (FGFR2) in mesenchymal–epithelial signaling during mouse organogenesis. Development 127, 483–492.

Ferguson, W.J., 1984. Epithelial–mesenchymal interactions during vertebrate palatogenesis. Curr. Top. Dev. Biol. 19, 137–164.

Fitzpatrick, D.R., Denhez, F., Kondaiah, P., Akhurst, R.J., 1990. Differential expression of TGF beta isoforms in murine palatogenesis. Development 109, 585–595.

Francis-West, P.H., Robson, L., Evans, D.J.R., 2003. Craniofacial development: the tissue and molecular interactions that control development of the head. In: Beck, F., Kriz, W., Marani, E., Sano, Y., Schoenwolf, G.C., Zilles, K. (Eds.), Adv. Anat. Embryol. Cell Biol. 169. Springer-Verlag, New York, pp. 69–73.

Gato, A., Martinez, M.L., Tudela, C., Alonso, I., Moro, J.A., Formoso, M.A., Ferguson, M.W., Martinez-Alvarez, C., 2002. TGF-beta (3)-induced chondroitin sulphate proteoglycan mediates palatal shelf adhesion. Dev. Biol. 250, 393–405.

Goumans, M.J., Valdimarsdottir, G., Itoh, S., Rosendahl, A., Sideras, P., ten Dijke, P., 2002. Balancing the activation state of the endothelium via two distinct TGF-beta type I receptors. EMBO J. 21, 1743–1753.

Griffith, C.M., Hay, E.D., 1992. Epithelial–mesenchymal transformation during palatal fusion: carboxyfluorescein traces cells at light and electron microscopic levels. Development 116, 1087–1099.

Halford, M.M., Armes, J., Buchert, M., Meskenaite, V., Grail, D., Hibbs, M.L., Wilks, A.F., Farlie, P.G., Newgreen, D.F., Hovens, C.M., Stacker, S.A., 2000. Ryk-deficient mice exhibit craniofacial defects associated with perturbed Eph receptor crosstalk. Nat. Genet. 25, 414–418.

Harada, H., Kettunen, P., Jung, H.S., Mustonen, T., Wang, Y.A., Thesleff, I., 1999. Localization of putative stem cells in dental epithelium and their association with Notch and FGF signaling. J. Cell Biol. 147, 105–120.

Harada, H., Toyono, T., Toyoshima, K., Yamasaki, M., Itoh, N., Kato, S., Sekine, K., Ohuchi, H., 2002. FGF10 maintains stem cell compartment in developing mouse incisors. Development 129, 1533–1541.

Hart, A., Papadopoulou, S., Edlund, H., 2003. *Fgf10* maintains notch activation, stimulates proliferation, and blocks differentiation of pancreatic epithelial cells. Dev. Dyn. 228, 185–193.

Hill, R.E., Jones, P.F., Rees, A.R., Sime, C.M., Justice, M.J., Copeland, N.C., Jenkins, N.A., Graham, E., Davidson, D.R., 1989. A new family of mouse homeobox containing genes: molecular structure, chromo-

somal location and developmental expression of *Hox7.1*. Genes Dev. 3, 26–37.

Igarashi, M., Finch, P.W., Aaronson, S.A., 1998. Characterization of recombinant human fibroblast growth factor (FGF)-10 reveals functional similarities with keratinocyte growth factor (FGF-7). J. Biol. Chem. 273, 13230–13235.

Jiang, R., Lan, Y., Chapman, H.D., Shawber, C., Norton, C.R., Serreze, D.V., Weinmaster, G., Gridley, T., 1998. Defects in limb, craniofacial, and thymic development in Jagged2 mutant mice. Genes Dev. 12, 1046–1057.

Kaartinen, V., Cui, X.M., Heisterkamp, N., Groffen, J., Shuler, C.F., 1997. Transforming growth factor-beta3 regulates transdifferentiation of medial edge epithelium during palatal fusion and associated degradation of the basement membrane. Dev. Dyn. 209, 255–260.

Kim, S.K., Hebrok, M., 2001. Intercellular signals regulating pancreas development and function. Genes Dev. 15, 111–127.

Lan, Y., Ovitt, C.E., Cho, E., Maltby, K.M., Wang, Q., Jiang, R., 2004. Odd-skipped related 2 (*Osr*2) encodes a key intrinsic regulator of secondary palate growth and morphogenesis. Development 131, 3207–3216.

Mansell, J.P., Kerrigan, J., McGill, J., Bailey, J., TeKoppele, J., Sandy, J.R., 2000. Temporal changes in collagen composition and metabolism during rodent palatogenesis. Mech. Ageing Dev. 119, 49–62.

Martínez-Álvarez, C., Bonelli, R., Tudela, C., Gato, A., Mena, J., O'Kane, S., Ferguson, M.W., 2000a. Bulging medial edge epithelial cells and palatal fusion. Int. J. Dev. Biol. 44, 331–335.

Martínez-Álvarez, C., Tudela, C., Perez-Miguelsanz, J., O'Kane, S., Puerta, J., Ferguson, M.W., 2000b. Medial edge epithelial cell fate during palatal fusion. Dev. Biol. 220, 343–357.

Martínez-Álvarez, C., Blanco, M.J., Pérez, R., Rabadán, M.A., Aparicio, M., Resel, E., Martínez, T., Nieto, M.A., 2004. Snail family members and cell survival in physiological and pathological cleft palates. Dev. Biol. 265, 207–218.

Miettinen, P.J., Chin, J.R., Shum, L., Slavkin, H.C., Shuler, C.F., Derynck, R., Werb, Z., 1999. Epidermal growth factor receptor function is necessary for normal craniofacial development and palate closure. Nat. Genet. 22, 69–73.

Min, H., Danilenko, D.M., Scully, S.A., Bolon, B., Ring, B.D., Tarpley, J.E., DeRose, M., Simonet, W.S., 1998. Fgf-10 is required for both limb and lung development and exhibits striking functional similarity to *Drosophila* branchless. Genes Dev. 12, 3156–3161.

Mori, C., Nakamura, N., Okamoto, Y., Osawa, M., Shiota, K., 1994. Cytochemical identification of programmed cell death in the fusing fetal mouse palate by specific labelling of DNA fragmentation. Anat. Embryol. (Berl.) 190, 21–28.

Morris-Wiman, J., Du, Y., Brinkley, L., 1999. Occurrence and temporal variation in matrix metalloproteinases and their inhibitors during murine secondary palatal morphogenesis. J. Craniofacial Genet. Dev. Biol. 19, 201–212.

Morris-Wiman, J., Burch, H., Basco, E., 2000. Temporospatial distribution of matrix metalloproteinase and tissue inhibitors of matrix metalloproteinases during murine secondary palate morphogenesis. Anat. Embryol. (Berl.) 202, 129–141.

Mustonen, T., Tummers, M., Mikami, T., Itoh, N., Zhang, N., Gridley, T., Thesleff, I., 2002. Lunatic fringe, FGF, and BMP regulate the Notch pathway during epithelial morphogenesis of teeth. Dev. Biol. 248, 281–293.

Norgaard, G.A., Jensen, J.N., Jensen, J., 2003. FGF10 signaling maintains the pancreatic progenitor cell state revealing a novel role of Notch in organ development. Dev. Biol. 264, 323–338.

Orioli, D., Henkemeyer, M., Lemke, G., Klein, R., Pawson, T., 1996. Sek4 and Nuk receptors cooperate in guidance of commissural axons and in palate formation. EMBO J. 15, 6035–6049.

Ornitz, D.M., Itoh, N., 2001. Fibroblast growth factors. Genome Biol. 2, 3005.1–3005.12. (REVIEWS3005).

Ohuchi, H., Hori, Y., Yamasaki, M., Harada, H., Sekine, K., Kato, S., Itoh, N., 2000. FGF10 acts as a major ligand for FGF receptor 2 IIIb in mouse multi-organ development. Biochem. Biophys. Res. Commun. 277, 643–649.

Papetti, M., Shujath, J., Riley, K.N., Herman, I.M., 2003. FGF-2 antagonizes the TGF-beta1-mediated induction of pericyte alpha-smooth muscle actin expression: a role for myf-5 and Smad-mediated signaling pathways. Invest. Ophthalmol. Visual Sci. 44, 4994–5005.

Park, W.Y., Miranda, B., Lebeche, D., Hashimoto, G., Cardoso, W.V., 1998. FGF-10 is a chemotactic factor for distal epithelial buds during lung development. Dev. Biol. 201, 125–134.

Pelton, R.W., Dickinson, M.E., Moses, H.L., Hogan, B.L., 1990. In situ hybridization analysis of TGF beta 3 RNA expression during mouse development: comparative studies with TGF beta 1 and beta 2. Development 110, 609–620.

Peters, H., Neubuser, A., Kratochwil, K., Balling, R., 1998. *Pax9*-deficient mice lack pharyngeal pouch derivatives and teeth and exhibit craniofacial and limb abnormalities. Genes Dev. 12, 2735–2747.

Rice, R., Spencer-Dene, B., Connor, E.C., Gritli-Linde, A., McMahon, A.P., Dickson, C., Thesleff, I., Rice, D.P.C., 2004. Disruption of *Fgf10*/*Fgfr2b*-coordinated epithelial–mesenchymal interactions causes cleft palate. J. Clin. Invest. 113, 1692–1770.

Satokata, I., Maas, R., 1994. Msx1 deficient mice exhibit cleft palate and abnormalities of craniofacial and tooth development. Nat. Genet. 6, 348–356.

Sekine, K., Ohuchi, H., Fujiwara, M., Yamasaki, M., Yoshizawa, T., Sato, T., Yagishita, N., Matsui, D., Koga, Y., Itoh, N., Kato, S., 1999. *Fgf10* is essential for limb and lung formation. Nat. Genet. 21, 138–141.

Shah, N.M., Groves, A.K., Anderson, D.J., 1996. Alternative neural crest cell fates are instructively promoted by TGFbeta superfamily members. Cell 85, 331–343.

Shuler, C.F., Guo, Y., Majumder, A., Luo, R.Y., 1991. Molecular and morphologic changes during the epithelial–mesenchymal transformation of palatal shelf medial edge epithelium in vitro. Int. J. Dev. Biol. 35, 463–472.

Shuler, C.F., Halpern, D.E., Guo, Y., Sank, A.C., 1992. Medial edge epithelium fate traced by cell lineage analysis during epithelial–mesenchymal transformation in vivo. Dev. Biol. 154, 318–330.

Suzuki, K., Yamanishi, K., Mori, O., Kamikawa, M., Anderson, B., Kato, S., Toyoda, T., Yamada, G., 2000. Defective terminal differentiation and hypoplasia of the epidermis in mice lacking the *Fgf10* gene. FEBS Lett. 481, 53–56.

Taya, Y., O'Kane, S., Ferguson, M.W., 1999. Pathogenesis of cleft palate in TGF-beta3 knockout mice. Development 126, 3869–3879.

Tudela, C., Formoso, M.A., Martinez, T., Perez, R., Aparicio, M., Maestro, C., Del Rio, A., Martinez, E., Ferguson, M., Martínez-Álvarez, C., 2002. TGF-beta3 is required for the adhesion and intercalation of medial edge epithelial cells during palate fusion. Int. J. Dev. Biol. 46, 333–336.

Unda, F.J., Martin, A., Hernandez, C., Perez-Nanclares, G., Hilario, E., Arechaga, J., 2001. FGFs-1 and -2, and TGF beta 1 as inductive signals modulating in vitro odontoblast differentiation. Adv. Dent. Res. 15, 34–37.

Valsecchi, C., Ghezzi, C., Ballabio, A., Rugarli, E.I., 1997. JAGGED2: a putative Notch ligand expressed in the apical ectodermal ridge and in sites of epithelial–mesenchymal interactions. Mech. Dev. 69, 203–207.

Weaver, M., Dunn, N.R., Hogan, B.L., 2000. *Bmp4* and *Fgf10* play opposing roles during lung bud morphogenesis. Development 127, 2695–2704.

Zhang, Z., Yu, X., Zhang, Y., Geronimo, B., Lovlie, A., Fromm, S.H., Chen, Y., 2000. Targeted misexpression of constitutively active BMP receptor-IB causes bifurcation, duplication, and posterior transformation of digit in mouse limb. Dev. Biol. 220, 154–167.

Zhang, Z., Song, Y., Zhao, X., Zhang, X., Fermin, C., Chen, Y., 2002. Rescue of cleft palate in Msx1-deficient mice by transgenic *Bmp4* reveals a network of BMP and Shh signaling in the regulation of mammalian palatogenesis. Development 129, 4135–4146.